Applied Geochemistry 87 (2017) 122–135

Contents lists available at ScienceDirect

Applied Geochemistry

journal homepage: www.elsevier.com/locate/apgeochem

Geochemical and lithium isotope tracking of dissolved solid sources in Permian Basin carbonate reservoir and overlying aquifer waters at an enhanced oil recovery site, northwest Texas, USA

Samantha Pfister[a], Rosemary C. Capo[a], Brian W. Stewart[a,*], G.L. Macpherson[b], Thai T. Phan[a,c], James B. Gardiner[a,c,d], J. Rodney Diehl[c], Christina L. Lopano[c], J. Alexandra Hakala[c]

[a] Department of Geology and Environmental Science, University of Pittsburgh, Pittsburgh, PA 15260, USA
[b] Department of Geology, 120 Lindley Hall, University of Kansas, Lawrence, KS 66045, USA
[c] Department of Energy-National Energy Technology Laboratory, 626 Cochrans Mill Rd., Pittsburgh, PA 15236, USA
[d] AECOM, 626 Cochrans Mill Rd., Pittsburgh, PA 15236, USA

ARTICLE INFO

Keywords:
Lithium isotopes
Produced water
Permian Basin
Ogallala aquifer
Total dissolved solids
Groundwater quality
Evaporite

ABSTRACT

Geochemistry and lithium isotope compositions (δ^7Li) of Permian Basin produced water and potable groundwater from overlying aquifers at an enhanced oil recovery (EOR) site in Gaines County, northwest Texas, are used to evaluate the effects of brine-groundwater-rock interactions, identify sources of dissolved solids, and characterize fluid flow and mixing processes. δ^7Li values (per mil deviations from the LSVEC standard ^{7}Li/^{6}Li ratio) for produced water from dolostones of the San Andres Formation ranged from +10.9 to +15.6‰ and fall within the range of formation waters from other sandstone/carbonate reservoir rocks in North America, Europe and the Middle East. These differ from produced waters from hydraulically fractured shales from the U.S. Appalachian Basin, including the Marcellus Shale, which tend to have lower δ^7Li values and higher Li/Cl, possibly indicating greater interaction with a terrigenous component. The San Andres produced water chemistry and Li isotope ratios are consistent with Neogene meteoric water interacting with marine and continentally-derived evaporites (e.g., portions of the Guadalupian Salado Formation), as well as other terrestrial sources along the flow path.

Groundwater from the Triassic Dockum Group-Santa Rosa aquifer (δ^7Li range of +20.6 to +23.5‰) is isotopically distinct from waters from the overlying Ogallala Formation (+10.6 to +16.5‰) and the deeper San Andres Formation, indicative of hydrologic isolation from both meteoric recharge and from deeper brines in the field area. In addition to tracking groundwater-brine mixing and water-rock interaction, temporal changes in the δ^7Li composition of deep groundwater in the study area has potential use in the early detection of upward or injection-induced brine migration, prior to its incursion into the sensitive overlying Ogallala aquifer.

1. Introduction

Waters co-produced with oil and gas extraction provide important information about downhole conditions in the reservoir, as well as the geologic and hydrologic history of the hydrocarbon-producing formation (e.g., Land and Prezbindowski, 1981; Walter et al., 1990; Chaudhuri et al., 1992; Hanor, 1994; Kharaka and Hanor, 2004; Engle et al., 2016). The Permian Basin in the western United States hosts a number of significant hydrocarbon reservoirs, and has been considered a potential site for high-level nuclear waste storage below low-permeability seals (Dutton, 1987), and more recently for long-term geologic carbon sequestration. High permeability rocks in the Permian Basin have been identified as potential carbon storage formations because of the low geothermal gradient in the area and close proximity to CO_2 pipelines (DOE-NETL, 2010). Carbon sequestration field studies have been conducted at a number of enhanced oil recovery (EOR) sites in the Permian Basin, including the SACROC field, the Mean's San Andres field, and the Wasson Denver project (Magruder et al., 1990; Stevens et al., 2001). Major structures within its boundaries include the Central Basin Platform, Delaware Basin, Midland Basin, and Northwest and Eastern Shelf (Fig. 1a). The Central Basin Platform is of particular economic importance due to its shallower oil plays in comparison to surrounding basins.

The High Plains-Ogallala aquifer, one of the largest freshwater

* Corresponding author.
E-mail address: bstewart@pitt.edu (B.W. Stewart).

http://dx.doi.org/10.1016/j.apgeochem.2017.10.013
Received 29 March 2017; Received in revised form 19 October 2017; Accepted 19 October 2017
Available online 21 October 2017
0883-2927/

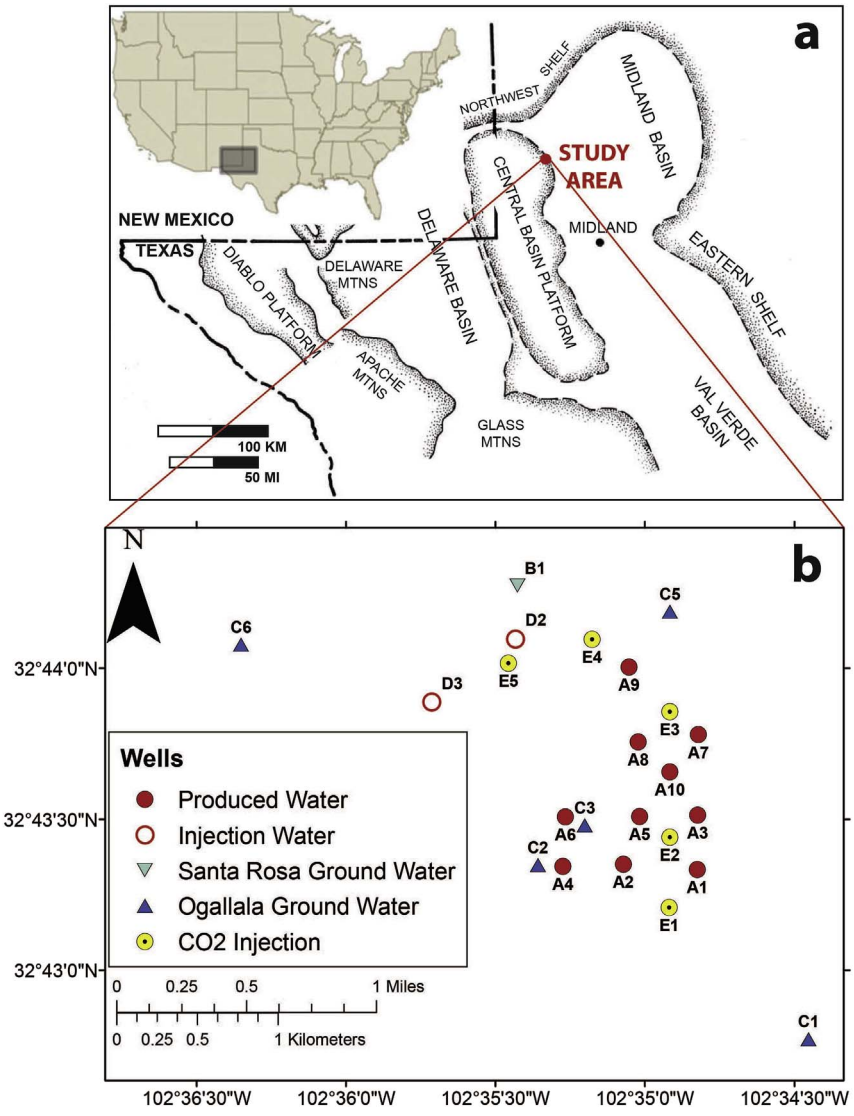

Fig. 1. **a**) Major Permian Basin structures in Texas and New Mexico. The produced waters for this study were sampled from oil wells located on the eastern flank of the Central Basin Platform and western edge of the Midland Basin (modified from Ward et al., 1986). **b**) Wells sampled for San Andres produced water (A), Santa Rosa groundwater (B), Ogallala groundwater (C), and injection water (D), as well as locations of CO_2 injection wells in the field area (E).

systems in the world and a critical water resource for much of the central and southwestern United States (e.g., Hornbeck and Keskin, 2014), overlies much of the Permian Basin hydrocarbon reservoir area. It is an important drinking water resource and the main source of agricultural water for a large part of the central U.S.A. Decreased recharge and increased agricultural use due to prolonged drought conditions, particularly in the southwest and including much of the Permian Basin, have accelerated depletion of this critical groundwater resource and affected water quality (Mehta et al., 2000; Gurdak et al., 2009; Scanlon et al., 2009; Venkataraman and Uddameri, 2012). Oil extraction from underlying reservoirs and the potential of long-term CO_2 storage beneath the aquifer have raised concerns about effects on water quality (Smyth et al., 2009). Although a number of studies have focused on potential environmental and health impacts of CO_2 injection-related metal mobilization on the aquifer, there still remains a need for detailed geochemical analysis and characterization of shallow groundwater and subsurface saline formation waters in the region (Carroll et al., 2010; Romanak et al., 2012).

Variations in the chemical and isotopic composition of formation and groundwater can be used as natural signatures of fluid migration, for early detection of saline fluids into overlying units, and as sensitive monitors of water-rock interaction. Natural isotopic tracers can be more sensitive to water quality changes than traditional elemental concentration and ratio indicators (Stewart et al., 1998; Banner, 2004; Kolesar Kohl et al., 2014). Temporal elemental and isotopic changes can be used for monitoring and source identification of fluid migration and water quality changes over both short (annual to decadal) and long (10^2–10^8 yr) timescales. The lithium (Li) isotopic measurements of produced water from oil and gas-bearing units have proven useful in determining the origin and evolution of basinal brines and identification of the effect of temperature on subsurface water-rock interactions (Chan et al., 2002; Millot et al., 2011; Macpherson et al., 2014; Phan et al., 2016). Lithium is an incompatible element that is generally removed from solids during water-mineral reactions, often accompanied by isotopic fractionation, and sometimes taken up by alteration minerals such as smectite (Tomascak et al., 2016) and the octahedral sites of illite (Williams and Hervig, 2005; Williams et al., 2012, 2015). Interpretations of Li concentration and isotope variability are attributed to diagenesis of silicate minerals (e.g., Millot et al., 2011) that dominate sedimentary basin lithology and undergo temperature-dependent reactions. Subsurface systems are usually rock-dominated with abundant reactive phases (Land and Macpherson, 1992), and the enrichment of Li concentrations over amounts predicted from source fluids repeatedly demonstrates this. The enrichment of Li in oilfield formation waters (Collins, 1975; Wilson and Long, 1993; Chan et al., 2002; Williams et al., 2015) suggests that it could be released from the source rock along with the hydrocarbons, and therefore Li isotopes may provide important information about catagenesis and the origin of

hydrocarbons and associated brines.

This work focuses on geochemical and lithium isotope compositions of produced waters and groundwaters from an EOR site in northwest Texas in the East Seminole oilfield within the San Andres Platform Carbonate play of the Permian Basin Central Basin Platform (Dutton et al., 2005). These measurements were used to identify and quantify fluid-rock interactions over different temporal scales and investigate produced/formation water pathways. The primary oil reservoir in the field consists of dolomitic rocks of the Upper Permian (Guadalupian) San Andres Formation, one of the most important oil reservoirs in the Permian Basin. Carbonate hydrocarbon reservoirs are targets of CO_2-enhanced hydrocarbon recovery methods in the Permian Basin and elsewhere because carbonate reservoirs have the porosity and permeability to accommodate CO_2 injection (Manrique et al., 2004; Bachu, 2008; Godec et al., 2013). We use these measurements to investigate formation water-groundwater-rock interactions and to discern sources of total dissolved solids (TDS). Furthermore, the presence of overlying aquifers, including the Tertiary Ogallala Formation of the Southern High Plains aquifer, provides an opportunity to test the ability of Li isotopes to identify sources of TDS in the Southern High Plains-Ogallala aquifer.

2. Geological setting and site description

The study area is an approximately 14 km^2 EOR site within the East Seminole oilfield, in Gaines County, Texas (Fig. 1). The oilfield is within the San Andres Platform Carbonate play of the Permian Basin Central Basin Platform (Dutton et al., 2005). Oil wells produce from depths of approximately 1625 m below the surface, tapping a 75 m thick section of the Upper San Andres Formation that consists of dolomitic carbonate rocks (Wang et al., 1998). These dolostones are characterized by high primary permeability and porosity, and were affected by diagenetic dolomitization, sulfate mineralization and karst-modification (Dutton, 1987; Bebout and Carlson, 1987; Ruppel and Cander, 1988). The San Andres dolostones and overlying evaporitic Ochoan Series of the Central Basin Platform form part of the Permian Composite carbon storage assessment unit (SAU) identified by the US Geological Survey as potentially suitable for carbon sequestration (Merrill et al., 2015). While adjacent oilfields have been periodically waterflooded and injected with CO_2 since the 1980s (Gray, 1989; Tennyson et al., 2012), CO_2 injection at the E. Seminole study site began in October 2013 and continued through the remainder of the study period. Waterflooding of the field occurred prior to and concurrent with CO_2 injection as part of secondary recovery.

Locally important aquifers overlying the San Andres Formation include the Santa Rosa Sandstone member of the Dockum Group (approximately 450 m depth) that is used primarily by the oil and gas industry in the field area. In addition, the overlying Ogallala Formation, part of the Southern High Plains aquifer, is an important source of irrigational and drinking water (Fahlquist, 2003). In Gaines County, the top of the Ogallala Formation is approximately 35–55 m beneath the surface and 45–60 m thick (Rettman and Leggat, 1966), with groundwater flow to the southeast. Stratigraphy and generalized lithologies are shown in Fig. 2. Compared to the northern part of the aquifer, Southern High Plains groundwater generally has higher TDS (median 800 mg L^{-1} in shallow groundwater) and arsenic concentrations that can exceed the USEPA drinking water standard of 10 μg L^{-1} (Mehta et al., 2000; Gurdak et al., 2009; Scanlon et al., 2009; Venkataraman and Uddameri, 2012).

3. Sampling and analytical methods

Water samples were collected during three sampling events from 18 wells in the study area (Fig. 1b): 10 producing wells (Wells A1-A10; 1615–1675 m depth); one industrial Santa Rosa aquifer well (Well B1, ~550 m depth); and three residential (C2, C3 and C5) and two irrigation (C1 and C6) Ogallala aquifer wells (45–75 m depth). Water samples were also collected from two injection wells (Wells D2 and D3). After the first sampling event, Well A10 was modified to allow injection of water and CO_2. Injection water consisted of groundwater from the Santa Rosa well (B1) mixed in a tank with recycled water from producing wells. The location of CO_2 injection wells (E1 through E5) are also shown in Fig. 1b.

The first set of samples was collected in June 2013, four months before CO_2 injection commenced in October 2013. The second and third sampling events occurred three months (January 2014) and seven months (May 2014) after the initiation of CO_2 injection. Because of ongoing oilfield operations, water samples were not available for some wells for all three sampling events; collection dates are noted in the data tables. At each well, pH was measured using a multi-meter (YSI® Instruments) with analytical accuracy of ± 0.2. All samples were collected at the wellhead into pre-rinsed carboys that were conditioned with sample water using new, pre-cleaned sample tubing for each sample. Produced water aliquots taken below the oil-water interface were passed though glass wool to qualitatively remove large particulates and oil, and then filtered through 0.45 μm high capacity filters (EnviroTech GWE) into acid-washed Nalgene HDPE bottles. Alkalinity was determined using Hach® titration methods, and calculated via the USGS Alkalinity Calculator (2012). Samples for major and trace cation and Li isotope analyses were preserved by acidification with ultrapure concentrated nitric acid to pH < 2. Samples for anion analysis were preserved by storage on ice followed by refrigeration in the lab.

Major and trace cations were analyzed using a Horiba Inductively Coupled Plasma-Optical Emission Spectrometer (ICP-OES; JY Ultima 2) and a VG Elemental Inductively Coupled Plasma-Mass Spectrometer (ICP-MS; PQII + XS) at the Kansas Geological Survey and University of Kansas, respectively. Anion concentrations were determined with a Dionex 4000i ion chromatograph (IC) equipped with an AS4a 4-mm analytical column and an AG4a guard column at the University of Kansas. Analytical accuracy and precision were determined by replicate analyses of samples, standards (ICP-OES: QCS-23; ICP-MS: Dionex 7 Anion Standard II (Br), QCS-23, and NIST1640a; IC: Dionex 7Anion Standard II); standards were matrix-matched to the samples. Calibration curves were created using mixtures of purchased (Spex Certiprep) single- and multi-element solutions. Based on the average of standard deviations for replicate samples, our estimate of analytical uncertainty is < 4% for all elements except Si (< 10%), K (< 17%), Ni (< 8%), Mo (< 14%), and U (< 8%).

Lithium separation and δ^7Li determinations were conducted at the University of Pittsburgh. Chromatographic separation of Li from the sample matrix for water samples, reference standards (Seawater NASS-6 and in-house brine standard WA-A25), sample replicates, and procedural blanks was conducted under clean lab conditions using a method described in detail by Phan et al. (2016), modified from Choi et al. (2013). Lithium yields and procedural blanks were determined on a NexION 300X ICP-MS. Lithium isotope compositions for samples with column yields ≥99% and blank ≤0.06% were measured on a Thermo Neptune Plus multicollector-ICP-MS (MC-ICP-MS) using a sample-standard bracketing technique and δ^7Li values were reported relative to the L-SVEC standard. The average δ^7Li of IRMM-016 measured over the course of this study was +0.2 ± 0.3‰ (2σ, n = 4) which is within analytical uncertainty of previous studies: for example, +0.1 ± 0.4‰ (Macpherson et al., 2014); +0.2 ± 0.2‰ (n = 22; Phan et al., 2016). The measured δ^7Li value for NASS-6 over the course of this study was 29.6 ± 2.2‰ (n = 6), which is within reported values for modern seawater (e.g., 29.3 ± 0.9‰, Nishio and Nakai, 2002; 31.3 ± 0.9‰, Pogge von Strandmann et al., 2010; 30.87 ± 0.15‰, Lin et al., 2016). In-house brine WA-A25 yielded δ^7Li of 9.56 ± 0.49‰ (n = 8), consistent with previous studies (Macpherson et al., 2014; Phan et al., 2016). Long-term instrumental reproducibility for δ^7Li is estimated to be ≤ 1‰ (2σ).

System	Series/Stage	Group/Formation	Lithology
Quaternary		*Alluvium*	silty sand
Tertiary	Upper	***Ogallala***	fluvial and lacustrine clastics
Cretaceous	Albian	*Fredericksburg*	limestone
		Paluxy	sandstone
Triassic	Upper	***Dockum Group / Santa Rosa Fm.***	fluvial-deltaic and lacustrine clastics
Permian	Ochoan	*Dewey Lake*	sandstone
		Rustler	salt, anhydrite
		Salado	salt
	Guadalupian	*Tansill*	anhydrite
		Yates	sandstone
		Seven Rivers	anhydrite
		Queen	sandstone
		Grayburg	dolostone, sandstone
		San Andres	dolostone with anhydrite
	Leonardian	*Clear Fork Group*	limestone-dolostone
		Wichita	
	Wolfcampian	*Wolfcamp*	shelf limestones, minor shale
Pennsylvanian	Virgilian	*Cisco*	
	Missourian	*Canyon*	
	Desmoinesian	*Strawn*	
	Atokan	*Atoka*	shale

Fig. 2. Stratigraphic column with generalized lithologies from the Pennsylvanian to the Quaternary in the Central Basin Platform (not to scale). The units from which formation waters were sampled are highlighted in bold. Modified from Stueber et al. (1998).

4. Results

4.1. Geochemistry of San Andres produced water

Major element data for San Andres produced and injection waters are presented in Table 1; trace element data are given in Table 2. The solutes in the produced waters are dominated by Na and Cl, with Ca^{2+} constituting approximately 20% of the total cation charge; sulfate (SO_4^{2-}) makes up approximately 25% of the anion charge (Fig. 3). Major element chemistry of the injection water is indistinguishable from the San Andres produced waters (Fig. 3), reflecting decades of pumping and reinjection of the same waters. Produced water from San Andres Formation wells are saline (TDS from 24,400 to 42,200 mg kg^{-1}) with pH ranging from 6.2 to 7.4. Sodium ranges from approximately 6300 to 13,900 mg kg^{-1} and Cl^- from approximately 10,400 to 20,600 mg kg^{-1}. Detectable hydrogen sulfide at the wellhead is indicative of reducing conditions in the formation. Alkalinity for produced and injection waters ranges from 1,110 to 1,800 mg kg^{-1} HCO_3^-; a slight increase in alkalinity over time is the only consistent time-dependent change in the major ions.

Barium concentrations (0.029–0.058 ppm) are lower than those found in Appalachian Basin produced waters by a factor of 10^4-10^5 (Chapman et al., 2012; Haluszczak et al., 2013), most likely due to the relatively high sulfate in the San Andres produced waters. These data extend the range of the inverse relation between barium and sulfate in deep fluids in the USA, thought to be controlled by the solubility of barite (Kharaka and Hanor, 2004). Concentrations of Sr are also lower than those in unconventional Appalachian Basin gas wells, even when normalized to TDS, but within the range of other deep fluids (Kharaka and Hanor, 2004). Concentrations of Ce, Co, Cr, Fe, La, Pb, V and Zn were below detection limits in all produced and injection water samples.

4.2. Geochemistry of Santa Rosa and Ogallala groundwaters

The major constituents of Ogallala and Santa Rosa groundwater samples are presented in Table 3. Ogallala aquifer groundwater pH is circumneutral (6.9–7.4), and TDS ranges between 797 and 2,200 mg kg^{-1}. Up to 50% of the total cation charge consisted of Na^+, with nearly equal amounts of Ca^{2+} and Mg^{2+} making up the remainder (Fig. 3). The total anion charge for most Ogallala samples consisted of less than 20% bicarbonate (HCO_3^-), and slightly more Cl^- than SO_4^{2-} (Fig. 3).

The high salinity of groundwater from the Santa Rosa aquifer in the area precludes its use for domestic or agricultural purposes. Total dissolved solid values for Santa Rosa well B1, locally used by the oil and gas industry, ranged from 4,520 to 4,650 mg kg^{-1}, and pH values ranged from 8.0 to 9.1. The dominant cation was Na^+, comprising more than 90% of the total cation charge, while SO_4^{2-} accounted for approximately 70% of the total anion charge (Fig. 3).

Trace element data for groundwater samples from Ogallala and Santa Rosa wells are presented in Table 4. Concentrations of Ce, La, and Zn were below the detection limit in all Ogallala water samples. Concentrations of Al, Rb, Ce, Co, Cr, Fe, La, Pb, V, and Zn were below detection limits in the Santa Rosa groundwater samples. Mean concentrations of Ba, Cu, Mn, Mo, and U in the Ogallala aquifer were similar to values reported by Stanton and Fahlquist (2006) for the southern High Plains aquifer in the same region. Barium concentrations in the Ogallala aquifer samples (0.037–0.088 ppm) were similar to or higher than those of the San Andres produced water, despite the significantly lower TDS in the Ogallala groundwaters. Although elevated, V concentrations of Ogallala groundwater in the study area (0.049–0.099 ppm) fall within the range of 0.009–0.532 mg L^{-1} found in other studies of the Southern High Plains Aquifer (Hopkins, 1993; Fahlquist, 2003). While the US Environmental Protection Agency (EPA) has not established a drinking water maximum contaminant level (MCL) for V, several states have set a health risk limit of 0.050 mg L^{-1} for drinking water (California Department of Public Health, 2010; Minnesota Department of Health, 2013). In 1999, V from an industrial leak contaminated some wells in Hockley County to the north, but locally V is associated with alteration of Cenozoic volcanic material (Potratz, 1980).

4.3. Lithium isotope results

Lithium isotope data for San Andres produced water, injection

Table 1
Major element geochemistry of produced and injection water samples. All analytes measured by ICP-OES except Br (ICP-MS), Cl and SO_4 (ion chromatograph), and HCO_3 (field titration).

Well	Date sampled[a]	pH	Na	K	Ca	Mg	Si	Cl	Br	SO_4	HCO_3	TDS[b]
			mg kg^{-1}									
San Andres Produced Water												
A1	2013–06	6.5	7130	162	1270	280	5.27	11,500	6.10	4750	1500	25,900
	2014–01	7.2									1630	
	2014–05	6.6									1630	
A2	2013–06	6.5	7310	167	1200	270	6.01	10,400	7.16	3760	1350	23,800
	2014–01	7.3	7310	375	1490	486	9.13	12,600	11.7	4550	1510	27,600
	2014-05(A)[c]	6.5	6510	122	1230	284	5.85	10,800	7.57	3860	1550	23,600
	2014-05(B)[c]		6310	141	1250	285	6.28	11,000	8.21	3890	1550	23,700
A3	2013–06	6.3	11,300	211	1450	334	12.2	18,100	8.49	4540	1600	36,800
	2014–01	6.8	10,500	326	1490	352	–[d]	15,800	10.4	4400	1600	33,700
	2014–05	6.5	9550	273	1450	326	6.00	15,800	11.1	4030	1650	32,300
A4	2013–06	6.3	8040	473	1410	421	9.72	13,600	11.4	4660	1370	29,300
	2014–01	6.2	7610	191	1250	301	–	12,600	8.01	4500	1410	27,200
A5	2014–01	7.3	9030	43.3	1210	260	–	10,400	7.01	4420	1440	26,200
	2014-05(A)[c]	6.9									1450	
A6	2013–06	6.4	7360	154	1330	250	5.52	10,700	6.27	4880	1110	25,300
	2014–01	6.5									1260	
A7	2013–06	6.3	10,500	246	1510	377	6.12	17,200	8.41	4110	1700	34,900
	2014–01	6.2	9600	294	1600	399	–	18,800	13.7	4150	1800	35,800
A8	2013–06	6.6	9610	225	1420	343	5.30	15,000	9.38	3680	1660	31,200
	2014–01	6.5									1570	
	2014–05	6.7									1630	
A9	2014-05(A)[c]	6.6	9210	458	1470	319	9.91	15,400	9.41	4140	1150	31,600
	2014-05(B)[c]		10,000	205	1460	308	6.56	15,700	9.29	4210		31,900
A10	2013–06	6.5	13,900	233	1570	358	4.24	20,600	6.72	4200	1290	41,500
Injection Water												
D2	2013–06	6.5	8450	193	1310	300	5.47	12,800	7.20	3930	1310	27,700
	2014–01	6.3	8760	195	1450	333	–	15,200	9.96	4370	1540	31,100
	2014–05	6.4	9540	238	1370	310	5.71	12,700	6.47	3900	1570	28,900
D3	2013–06	6.4	6670	181	1240	269	5.28	11,600	4.86	3980	1360	24,600
Min. detection limit:			*0.6*	*3.4*	*1.1*	*1.8*	*0.8*	*409.0*	*1.4*	*300*		

[a] Year and month.
[b] Total dissolved solids calculated from the sum of the measured cations and anions. TDS for sample A9-2014-05(B) based on alkalinity from field duplicate.
[c] (A) and (B) refer to field duplicate samples.
[d] Hyphen (−) indicates below detection limit.

water, Ogallala groundwater, and Santa Rosa Formation groundwater are presented in Table 5. The total range of δ^7Li in the San Andres produced waters is +10.9 to +15.6‰, which is very comparable to the range in the Ogallala aquifer samples (+10.6 to +16.5‰). In contrast, the Santa Rosa groundwater samples yield δ^7Li values in the range of +20.6 to +23.5‰, significantly higher than the Ogallala or San Andres values. San Andres waters have higher Li concentrations (1.4–2.4 mg kg^{-1}) than Santa Rosa or Ogallala waters, both of which fall within the range of 0.13–0.28 mg kg^{-1}.

Nearby undiluted San Andres formation waters, also from the eastern flank of the Central Basin Platform, have higher concentrations of Li (up to 7.3 mg L^{-1}, average 3.9 mg L^{-1}; Stueber et al., 1998), than the produced waters from the East Seminole site. The lower concentrations at East Seminole are likely the result of dilution resulting from waterflooding related to EOR. Injection water is composed of a mixture of recycled San Andres produced water and Santa Rosa groundwater, each of which has a significantly different Li/Cl ratio and Li isotope composition (Fig. 4). This difference in δ^7Li could conceivably shift the isotopic composition of waters produced from the San Andres Formation after waterflooding. Assuming that the undiluted formation water has concentrations similar to those found by Stueber et al. (1998) and isotope ratios similar to those from this study, we can calculate how much Santa Rosa groundwater would need to be added in order to change the δ^7Li of the produced waters. The mixing curves (Fig. 5) indicate that in order to generate a measurable shift in δ^7Li, Santa Rosa groundwater would have to make up $\geq \sim 75\%$ of the mixture, which is higher than is suggested by the most dilute San Andres waters (Fig. 5). Therefore, we assume that the δ^7Li values of San Andres produced water after waterflooding are only negligibly different from those of the original formation water.

The range of δ^7Li values measured in San Andres produced waters (Fig. 6) is similar to those reported from conventional (primarily oil) wells from the Gulf Coast Sedimentary Basin (Macpherson et al., 2014), and the Appalachian Basin (Macpherson et al., 2014; Warner et al., 2014; Phan et al., 2016), while it falls in between conventional produced water values reported for the Paris Basin (Millot et al., 2011), and the Heletz-Kokhav oil field, Israel (Chan et al., 2002). Produced waters from unconventional gas wells in the Appalachian Basin, including the Marcellus Shale (Macpherson et al., 2014; Warner et al., 2014; Phan et al., 2016), have generally lower δ^7Li values than those of the San Andres produced waters (Fig. 6). San Andres Li concentrations are lower than most of these oilfield brines, again most likely due to waterflooding at the East Seminole site, but still well above that of seawater.

5. Discussion

5.1. Sources of major dissolved constituents in San Andres produced waters

Permian Basin formation water chemistry can reflect a complex history of seawater evaporation, ion exchange, halite dissolution, dolomitization, and precipitation of gypsum (Dutton, 1987; Stueber et al.,

Table 2
Trace metal concentrations (by ICP-MS) of produced and injection water samples.

Well	Date Sampled[a]	Li	B	Al	Mn	Ni	Cu	Rb	Sr	Ba	U
		mg kg^{-1}									
San Andres Produced Water											
A1	2013–06	1.77	3.46	–[c]	0.0151	–	–	0.172	26.7	0.0421	–
	2014–01	1.84		–	–	0.193	–	0.193		0.0331	0.0010
	2014–05	1.78		–	0.104	0.142	0.0168	0.185		0.0319	–
A2	2013–06	1.81	3.43	–	0.00926	–	–	0.189	26.1	0.0303	–
	2014–01	1.93	4.06	–	0.0446	–	–	0.209	28.5	0.0344	0.0021
	2014-05(A)[b]	1.72	3.37	–	0.0122	0.201	–	0.184	25.9	0.0285	–
	2014-05(B)[b]	1.74	3.42	0.0312	0.0125	0.210	0.0164	0.187	26.1	0.0293	–
A3	2013–06	2.07	4.15	0.406	0.0223	–	–	0.213	32.1	0.0538	–
	2014–01	1.91	3.63	–	0.0194	0.0883	–	0.203	31.6	0.0413	0.0013
	2014–05	1.96	3.81	0.0127	0.156	0.105	–	0.211	31.5	0.0415	–
A4	2013–06	1.62	4.27	–	0.0789	0.269	–	0.197	30.4	0.0510	–
	2014–01	1.60	3.27	–	0.0197	0.209	–	0.177	27.5	0.0300	0.00082
A5	2014–01	1.47	2.92	–	0.648	0.227	–	0.133	24.2	0.0294	0.0012
	2014-05(A)[b]	1.40		–	0.317	0.154	–	0.128		0.0364	–
	2014-05(B)[b]			–	0.314	0.186	–	0.130		0.0370	–
A6	2013–06	1.64	3.48	–	0.0139	–	–	0.173	26.6	0.0452	–
	2014–01			–	0.00804	0.356	–	0.179		0.0313	0.00072
A7	2013–06	2.36	4.15	0.0740	0.0313	–	–	0.273	35.6	0.0479	–
	2014–01	2.27	4.07	–	–	0.0816	–	0.276	35.5	0.0375	0.00092
A8	2013–06	2.36	4.11	–	0.0460	–	–	0.272	34.8	0.0461	–
	2014–01	1.63		–	0.0406	0.116	–	0.250		0.0363	0.0011
	2014–05	2.22		–	0.0133	0.0945	–	0.253		0.0358	–
A9	2014-05(A)[b]	1.41	4.64	–	0.112	–	–	0.217	36.8	0.0553	–
	2014-05(B)[b]	1.38	4.01	–	0.106	0.113	–	0.213	33.9	0.0556	–
A10	2013–06	1.88	4.38	–	0.0459	–	–	0.179	33.4	0.0573	–
Injection Water											
D2	2013–06	1.80	3.79	–	0.0840	–	–	0.202	29.2	0.0487	–
	2014–01	1.91	3.77	–	0.0363	0.0796	–	0.229	32.8	0.0362	0.0010
	2014–05	1.78	3.58	–	0.237	0.0930	–	0.199	30.1	0.0335	–
D3	2013–06	1.69	3.21	–	0.0279	–	–	0.170	25.9	0.0434	–
Min. detection limit:		*0.003*	*0.66*	*0.014*	*0.006*	*0.068*	*0.016*	*0.006*	*0.007*	*0.0009*	*0.0008*

[a] Year and month.
[b] (A) and (B) refer to field duplicate samples.
[c] Hyphen (–) indicates below detection limit.

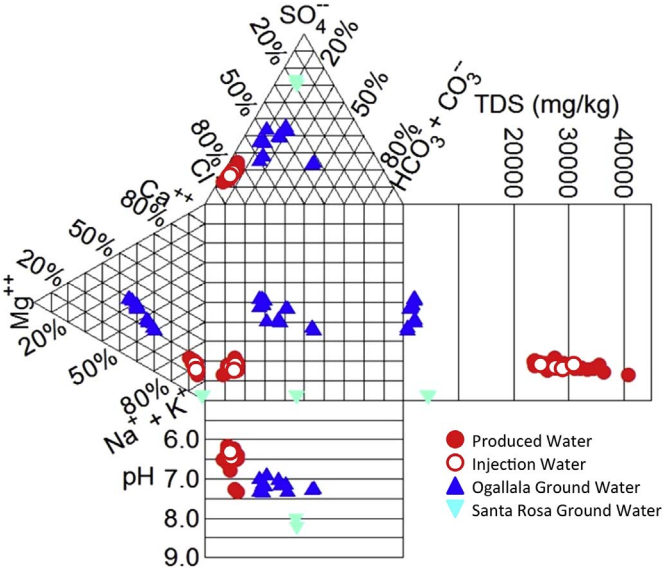

Fig. 3. Durov plot showing major chemistry variations of all well water and injection water samples analyzed in this study.

1998; Barnaby et al., 2004; Engle and Blondes, 2014; Engle et al., 2016). Bein and Dutton (1993) suggest that Ca-Cl type brines in the Permian basin are modified depositional waters (approximately the same age as their host unit), while Na-Cl type brines represent relatively recent (5–10 Ma) meteoric waters that have interacted with halite and gypsum. Within the Central Basin Platform, Stueber et al. (1998) suggest that the San Andres formation waters are primarily meteoric in origin with subsequent halite (and minor K-rich salt) dissolution responsible for salinity, based on the expected variation of Na/Br and Cl/Br in response to seawater evaporation and halite dissolution (Walter et al., 1990). A similar origin was suggested by Engle et al. (2016) for Guadalupian produced waters from the eastern Central Basin Platform. In Fig. 7, we compare San Andres produced waters from East Seminole to undiluted San Andres formation waters reported by Stueber et al. (1998). The East Seminole waters also fall along the halite evaporation trend, extending to significantly higher Na/Br and Cl/Br values than those measured by Stueber et al. (1998). This could be due to (1) additional halite dissolution induced by waterflooding (adding Na and Cl but not Br), or (2) lateral variations in the extent of halite dissolution by meteoric water farther from the recharge area. The Li/Cl ratios of the diluted San Andres produced waters (Fig. 4) overlap almost completely with those of undiluted San Andres waters (Stueber et al., 1998). Dilution from waterflooding should more strongly affect Cl concentrations than Li concentrations, because the diluting Santa Rosa waters have a relatively high Li/Cl. However, the dilution could be offset by the additional dissolution of halite, which adds Cl but not Li. These

Table 3
Major element geochemistry of groundwater samples. All analytes measured by ICP-OES except Br (ICP-MS), Cl and SO_4 (ion chromatograph), and HCO_3 (field titration).

Well	Well type[a]	Depth (m)	Date sampled[b]	pH	Na	K	Ca	Mg	Si	Cl	Br	SO_4	HCO_3	TDS[c]
					mg kg^{-1}									
Santa Rosa Formation Groundwater														
B1	I	460	2013–06	8.0	1410	7.09	24.7	11.4	5.16	403	0.891	2280	371	4330
			2014-01(A)[d]	9.1									433	
			2014-05(A)[d]	8.2	1380	5.51	19.0	10.8	4.28	442	1.70	2280	459	4370
			2014-05(B)[d]		1410	5.43	19.1	10.9	4.33	443	1.70	2290		4190
Min. detection limit:					*0.07*	*0.4*	*0.1*	*0.2*	*0.09*	*38*	*0.2*	*28*		
Ogallala Aquifer														
C1	A	53	2013–06	6.9	320	9.15	151	129	35.4	496	2.03	611	171	1840
			2014–01	7.2	323	8.88	150	128	34.2	495	1.86	625	385	1960
			2014–05	7.1	311	9.23	155	133	35.6	523	1.64	649	371	2010
C2	R	47	2013–06	7.3	134	4.33	49.3	41.8	24.3	126	0.498	124	291	649
			2014–05	7.3	129	4.51	52.1	44.0	24.6	149	0.429	132	321	695
C3	R	55	2013–06	7.0	172	9.76	130	113	32.4	499	1.79	284	221	1350
			2014–01	7.4	186	9.81	153	128	35.6	567	2.17	372	275	1590
			2014–05	7.1	194	9.99	152	129	35.8	560	1.64	376	270	1600
C5	R	55	2013–06	7.3	191	12.6	191	176	31.4	671	2.54	604	203	1990
			2014-01(A)[d]	7.2	191	13.7	194	173	33.9	673	2.65	610	235	2010
			2014–05	7.2	209	13.6	195	172	30.5	669	2.07	620	286	2060
C6	A	46	2013–06	7.2	150	8.30	106	95.3	26.3	240	1.25	403	212	1140
			2014–05	7.4	160	8.54	112	97.0	25.5	280	1.23	431	272	1250
Min. detection limit:					*0.2*	*0.03*	*0.006*	*0.003*	*0.03*	*8*	*0.01*	*6*		

[a] Industrial (I), residential (R) or agricultural (A).
[b] Year and month.
[c] Total dissolved solids calculated from the sum of the measured cations and anions. TDS for sample B1-2014-05(B) based on alkalinity from field duplicate.
[d] (A) and (B) refer to field duplicate samples.

Table 4
Trace metal concentrations (by ICP-MS) of groundwater samples.

Well	Date Sampled[a]	Li	B	Al	V	Cr	Mn	Fe	Ni	Cu	Rb	Sr	Mo	Ba	Pb	U
		mg kg^{-1}														
Santa Rosa Formation Groundwater																
B1	2013–06	0.236	1.30	–[c]	–	–	0.0630	–	0.622	–	–	0.838	0.0377	0.00648	–	0.00039
	2014-01(A)[b]	0.256		–	–	–	0.0426	–	1.28	–	–		0.0364	0.00472	–	0.00029
	2014-01(B)[b]	–		–	–	–	0.136	–	1.22	0.00637	–		0.0373	0.00738	–	0.00032
	2014-05(A)[b]	0.235	1.34	–	–	–	0.102	–	0.868	–	–	0.813	0.0379	0.00685	–	0.00024
	2014-05(B)[b]	0.228	1.34	–	–	–	0.100	–	0.803	–	–	0.821	0.0461	0.00652	–	0.00026
Min. detect. limit:		*0.001*	*0.08*	*0.005*	*0.01*	*0.02*	*0.002*	*0.07*	*0.01*	*0.002*	*0.00070*	*0.001*	*0.0012*	*0.00009*	*0.00026*	*0.0001*
Ogallala Aquifer																
C1	2013–06	0.271	0.979	0.00655	0.600	–	0.0163	–	0.0246	–	–	4.08	0.0262	0.0388	–	0.0170
	2014–01	0.272	0.968	–	0.497	–	0.0200	–	0.0296	–	–	4.08	0.0081	0.0376	–	0.0142
	2014–05	0.281	1.00	–	0.685	0.027	0.0255	–	0.0193	–	–	4.23	–	0.0378	–	0.0155
C2	2013–06	0.131	0.349	0.00202	0.811	–	0.00067	–	–	0.00981	–	1.38	0.0069	0.0559	0.00064	0.00664
	2014–05	0.126	0.344	–	0.765	–	0.00063	–	–	0.00218	–	1.44	0.0079	0.0643	–	0.00636
C3	2013–06	0.251	0.361	0.00086	0.693	0.032	–	–	–	0.00390	0.00025	3.45	0.0041	0.0625	0.00020	0.00813
	2014–01	0.268	0.422	–	0.550	0.0482	0.00055	–	–	0.00601	0.00015	3.81	0.0037	0.0644	–	0.00810
	2014–05	0.250	0.421	–	0.548	0.036	–	–	–	0.0219	–	3.86	0.0045	0.0752	0.00042	0.00811
C5	2013–06	0.256	0.614	0.00234	0.877	0.035	0.00919	0.209	0.00869	0.0103	0.00066	5.71	0.0061	0.0838	0.00062	0.0103
	2014-01(A)[b]	0.264	0.607	0.734	0.989	0.044	0.00777	0.536	–	0.0107	0.00174	5.85	0.0061	0.0879	0.00015	0.0100
	2014–05	0.248	0.603	–	0.833	0.038	0.0140	–	0.0117	0.00210	0.00056	5.81	0.0070	0.0811	–	0.00994
C6	2013–06	0.200	0.327	0.00253	0.915	–	0.00461	–	0.00903	0.00415	–	3.18	0.0085	0.0458	0.00018	0.00971
	2014–05	0.181	0.334	–	0.814	–	0.00201	–	0.00962	0.00455	–	3.25	0.0093	0.0543	–	0.0101
Min. detect. limit:		*0.0002*	*0.02*	*0.001*	*0.006*	*0.02*	*0.0003*	*0.005*	*0.006*	*0.0005*	*0.0002*	*0.0037*	*0.0037*	*0.00004*	*0.0001*	*0.00003*

[a] Year and month.
[b] (A) and (B) refer to field duplicate samples.
[c] Hyphen (–) indicates below detection limit.

Table 5
Lithium isotope data for all samples.

Well	Date sampled[a]	Li, mmol kg^{-1}	δ^7Li	Replicates[b]	
San Andres Produced Water					
A1	2014–05	0.257	14.3	14.0	
A2	2013–06	0.261	14.8		
	2014–01	0.278	15.7	15.4	
	2014-05(A)[c]	0.248	15.3		
	2014-05(B)[c]	0.250	14.2		
A3	2013–06	0.298	12.8	12.8	
	2014–01	0.275	14.0		
	2014–05	0.282	13.8	13.4	
A4	2013–06	0.233	13.6	12.8	12.7
	2014–01	0.231	14.0		
A5	2014–01	0.212	15.3		
	2014-05(A)[c]	0.202	13.9		
	2014-05(B)[c]	0.209	14.9	14.8	
A6	2013–06	0.236	15.6		
	2014–01	0.235	14.8	14.3	
A7	2013–06	0.340	15.3		
	2014–01	0.327	13.4		
A8	2013–06	0.340	13.1		
	2014–01	0.305	13.6		
	2014–05	0.320	12.3	12.5	
A9	2014-05(A)[c]	0.203	11.4	10.9	
	2014-05(B)[c]	0.198	12.3		
A10	2013–06	0.271	14.8		
Injection Water					
D2	2013–06	0.259	11.9	12.5	
	2014–01	0.275	11.5		
	2014–05	0.256	11.9		
D3	2013–06	0.244	14.5	14.1	
Santa Rosa Formation Groundwater					
B1	2013–06	0.0340	20.7	20.6	
	2014-01(A)[c]	0.0369	23.5		
	2014-01(B)[c]	0.0383	22.8	22.7	
	2014-05(A)[c]	0.0339	22.3	21.1	
	2014-05(B)[c]	0.0328	21.7	21.5	
Ogallala Aquifer					
C1	2013–06	0.0391	15.7		
	2014–01	0.0392	16.5		
C2	2013–06	0.0189	11.6		
	2014–05	0.0182	11.4	11.6	11.1
C3	2013–06	0.0361	13.3		
	2014–01	0.0386	14.6	14.2	14.0
	2014–05	0.0360	14.7		
C5	2013–06	0.0369	14.8		
	2014–01	0.0380	14.7		
	2014–05	0.0357	15.0	15.0	
C6	2013–06	0.0288	11.6	12.5	11.5
	2014–05	0.0261	10.6		

[a] Year and month.
[b] Replicates represent separate passes through Li columns.
[c] (A) and (B) refer to field duplicate samples.

observations suggest that waterflooding most likely led to additional halite dissolution, and that Li, but not Cl, behaved conservatively during the waterflooding events.

Because the San Andres is a dolomitic reservoir, it is expected that the dolomite host rock itself will exert some control on water chemistry. Molar concentrations of Ca are in excess of Mg for all produced water samples, but Ca and Mg vary with a slope very close to unity when combined with the eastern Platform data (Fig. 8). We suggest that this covariation reflects dissolution of dolomite host rock, with the "excess" Ca (the intercept at Mg = 0 on Fig. 8) being inherited from interaction of meteoric waters with gypsum/anhydrite evaporite units, or from dissolution of sulfates that occur within the dolostones (Ramondetta, 1982).

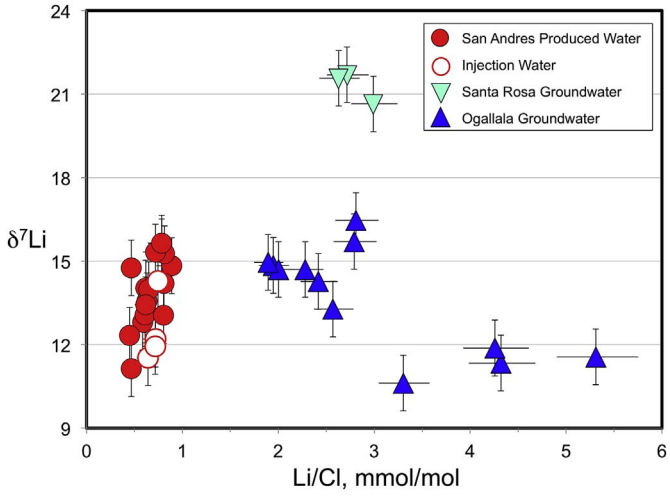

Fig. 4. Lithium isotopes (δ^7Li) plotted against Li/Cl ratios for all samples analyzed in this study. Error bars on δ^7Li values represent the estimated long-term external reproducibility (± 1‰).

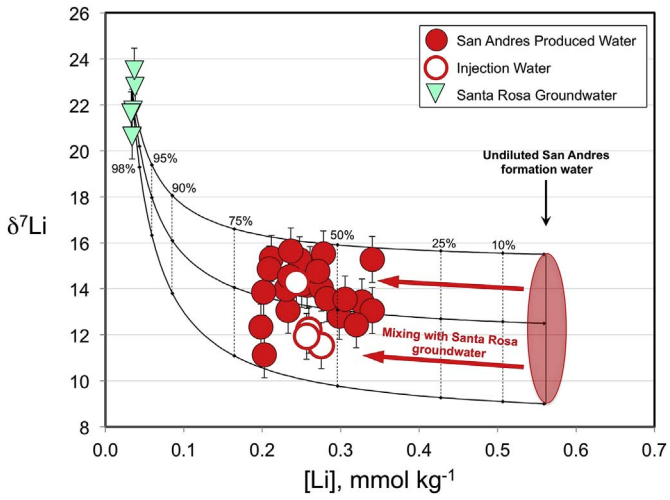

Fig. 5. Mixing curves between two end members: (1) Santa Rosa groundwater values from this study and (2) undiluted San Andres Formation water (red shaded region) from Stueber et al. (1998), using their Li concentrations and assuming the same range of δ^7Li values for their samples as measured in this study. Percentages represent the fraction of added Santa Rosa groundwater. The San Andres produced waters from this study (filled circles) fall within a range defined by 40–70% addition of Santa Rosa water during waterflooding, which would have had only minimal effect on their δ^7Li values. (For interpretation of the references to colour in this figure legend, the reader is referred to the web version of this article.)

5.2. Sources of Li in San Andres produced waters

5.2.1. Interaction of formation waters with marine evaporite minerals

Major element data discussed in Section 5.2 and isotope data from Stueber et al. (1998) and Barnaby et al. (2004) strongly suggest that San Andres waters in the Central Basin Platform are primarily meteoric in origin, with the recharge originating in southeastern New Mexico. The bulk of the TDS appears to have originated from dissolution of evaporite minerals along the flowpath, including the extensive Upper Permian Salado evaporite sequence; therefore, we will consider the possibility that this is the origin of the Li in San Andres waters. Marine evaporites would inherit δ^7Li values similar to those of the seawater at the time of precipitation. Misra and Froelich (2012) extended the marine δ^7Li record back to about 70 Ma using planktonic foraminifera from eight deep-sea cores, and found secular variations with δ^7Li values as low as +20 at 60 Ma. There are currently no data to directly support

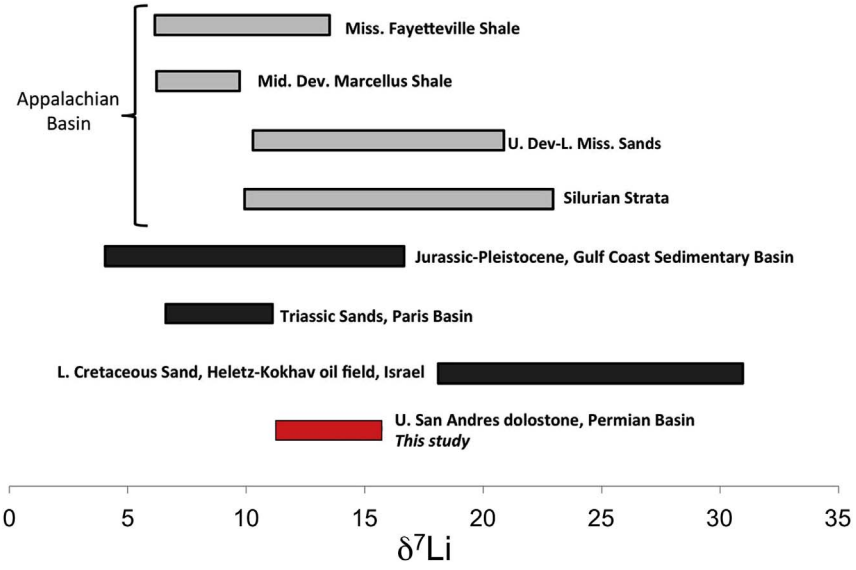

Fig. 6. δ^7Li values from this study compared to published formation waters from other hydrocarbon producing basins. Data are from Chan et al. (2002), Millot et al. (2011), Macpherson et al. (2014), Warner et al. (2014), and Phan et al. (2016).

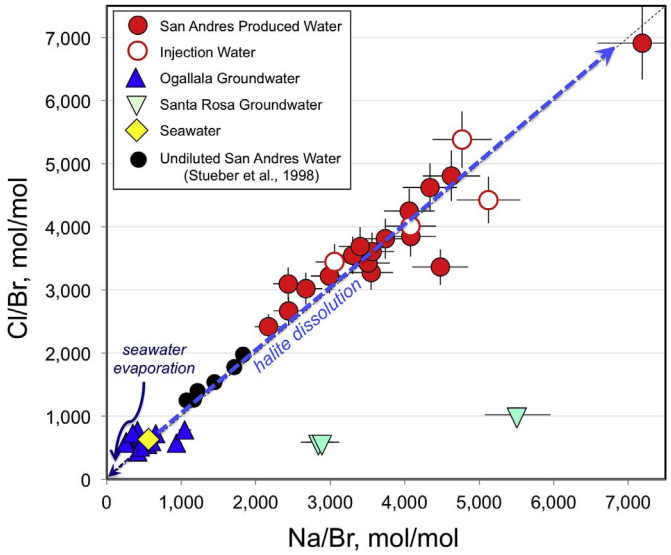

Fig. 7. Molar Cl/Br vs. molar Na/Br ratios for samples in this study compared to the range of undiluted San Andres formation waters from Stueber et al. (1998; uncertainties not reported). The halite dissolution trend (blue dashed line) extends from modern seawater along a positive slope of 1, while seawater evaporation is a trajectory from modern seawater toward the origin (Walter et al., 1990). (For interpretation of the references to colour in this figure legend, the reader is referred to the web version of this article.)

Permian seawater δ^7Li values as low as the +10 to +16‰ range observed in the San Andres produced water, although the similarities between the seawater-δ^7Li curve and the seawater-$^{87}Sr/^{86}Sr$ curve, with both δ^7Li and $^{87}Sr/^{86}Sr$ responding to differential rates of seafloor spreading and continental weathering, suggest that these lower values are within the realm of possibility for seawater during the time of deposition of the Salado evaporites.

However, while the δ^7 Li values of San Andres waters do not rule out a marine evaporite source, there are some additional mass-balance restrictive constraints. Lithium concentrations in evaporitic calcium sulfates (anhydrite and gypsum) are likely very low because of the relatively pure compositions of these minerals and the poor correspondence in size and charge between Li^+ and Ca^{2+}. Assuming that Li^+ and Br^- are both largely excluded from other evaporite minerals such as halite during seawater evaporation (e.g., Hermann, 1980; McCaffrey et al., 1987; Tomascak et al., 2016), residual fluids should have Li/Br ratios close to that of seawater (0.030 M/M; Millero and Sohn, 1992). The molar Li/Br ratios from San Andres produced waters range from 1.6 to 3.3, suggesting either (1) Br was incorporated into one or more minerals during seawater evaporation, or (2) Li was added later to these waters. Because Br is strongly excluded from marine evaporite minerals (Stoessell and Carpenter, 1986; McCaffrey et al., 1987; Walter et al., 1990), scenario (1) is unlikely. If scenario (2) is the case, then only 1–2% of the Li in the produced waters is derived from marine evaporite deposits or evaporated seawater, and the remaining 98–99% was added from other sources. While dissolution of marine evaporites was likely an important source of solutes (e.g., Na, Cl) in San Andres produced waters, we conclude that it contributed only a small fraction of the lithium.

5.2.2. *Continentally-derived sources*

Lowenstein (1988) interpreted the Salado evaporites as a combination of seawater evaporation ("Type I") and continental-dominated saline lake sequences ("Type II"). While the former appears to be an unlikely source of Li for the San Andres produced waters due to the exclusion of Li from marine evaporite minerals, continental saline lake sequences could provide significant amounts of Li. For example, lacustrine evaporites from Searles Lake, California, contain up to 0.06% (600 ppm) Li in some units (Smith et al., 1983), and playas from the western U.S. were found to contain up to ~700 ppm leachable Li (Araoka et al., 2013).

Alternate sources for Li, contributed during diagenesis after sediment deposition, include the numerous bentonites in the stratigraphic section. For example, the unconformity between the top of the San Andres and the overlying Whitehorse Group (or the top of the San Andres, according to Todd, 1976) is marked by an extensive bentonite marker bed. There are also several bentonites in stratigraphically higher units, and silicic Tertiary volcanics in the Davis Mountains to the southwest. Although the Li and δ^7Li systematics of these materials have not been investigated, the smectite clays that constitute most bentonites are likely to contain exchangeable Li in interlayer sites (Williams and Hervig, 2005; Vigier et al., 2008; Williams et al., 2013), and this could either be released into an interacting fluid or incorporated into the octahedral sites of neoformed clay minerals such as illite. In the latter case, the smectite would be only a minor source of Li in the interacting fluid.

Other types of continentally-derived Li that could contribute to San Andres produced waters contain a wide range of δ^7Li values (including but not restricted to the values measured in the produced waters), based on δ^7Li analyses of stream waters and groundwater (Kloppmann et al., 2009; Millot et al., 2010; Pogge von Strandmann et al., 2010; Tipper

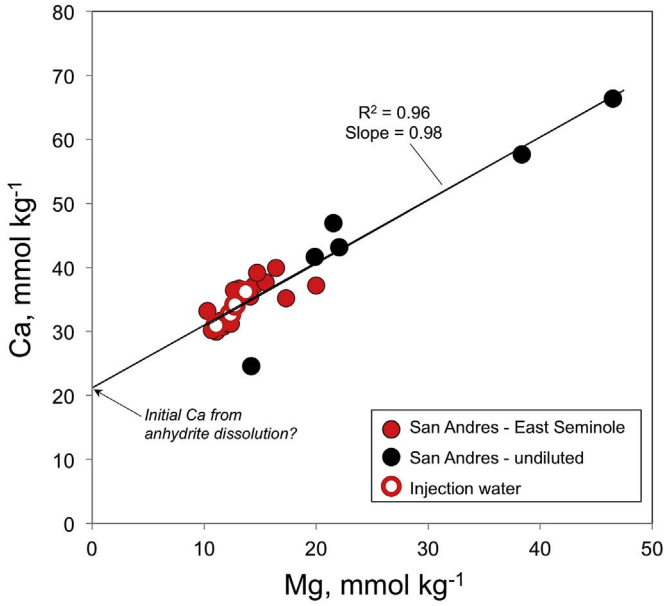

Fig. 8. Ca vs. Mg for San Andres produced and injection water from this study, and undiluted San Andres produced water from Stueber et al. (1998). The slope of ~1 suggests control of Ca and Mg by interaction of formation waters with dolomite in the reservoir.

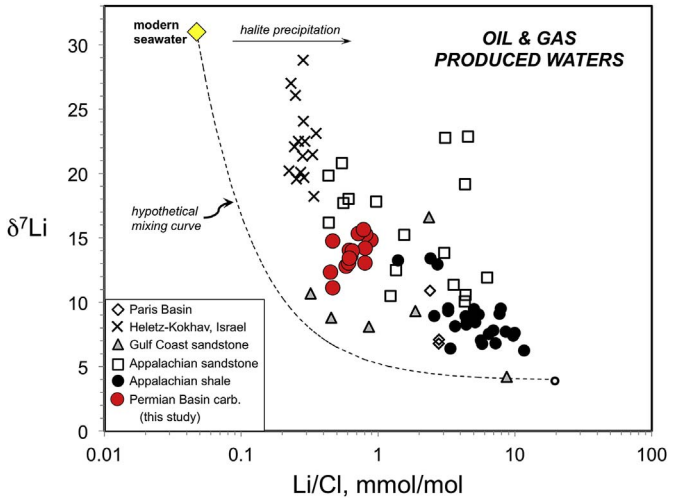

Fig. 9. δ^7Li values vs. molar Li/Cl for samples analyzed in this study (solid red circles) and published formation waters (data from same sources as Fig. 7). Modern seawater (yellow diamond) is shown for comparison (seawater [Li] from Li, 1991). The dashed mixing curve shows the trajectory for seawater mixing with a hypothetical low- δ^7Li, high Li/Cl source. We note that neither end member for the example mixing curve is well constrained, as past seawater δ^7Li could have been significantly different, and the terrestrial source is likely to be variable; however, the curve shows the expected trajectory for a two-component mixing in this system. The "halite precipitation" arrow shows the direction a brine would shift in response to crystallization of halite. (For interpretation of the references to colour in this figure legend, the reader is referred to the web version of this article.)

et al., 2012; Meredith et al., 2013; Dellinger et al., 2014; Bagard et al., 2015; Pogge von Strandmann et al., 2017). A significant contribution of Li from hydrothermal processes in the source region or flow path, as seen in salt pans from the Central Andes (Godfrey et al., 2013), would most likely have had the effect of lowering the δ^7Li of San Andres produced waters (Tomascak et al., 2003; Millot et al., 2012).

5.2.3. Dolomitic host rock

Because the San Andres formation waters are hosted in a carbonate reservoir, interaction with the calcitic/dolomitic host rocks could modify the Li isotope composition. Marine carbonate incorporates Li that is 2–4‰ lighter (lower δ^7Li) than the water from which it precipitates (Marriott et al., 2004; Pogge von Strandmann et al., 2013). The concentration of Li in marine carbonate is low (typically 0.5–1.5 ppm in calcite; Marriott et al., 2004). The relatively high Li/Ca (0.0009–0.0017) and Li/Mg (0.0038–0.0069) ratios in the San Andres water argue against a significant component from carbonate dissolution; even a dolomite with 10 ppm Li would yield Li/Ca of only 0.00005 and Li/Mg of only 0.00008. Thus water-carbonate interaction is unlikely to have played a significant role in modifying the δ^7Li of San Andres formation waters.

5.2.4. Comparison to other produced/formation waters

As indicated in Fig. 6, δ^7Li values in San Andres produced waters fall within the broader range of values that have been measured in oil and gas produced waters to date. The waters can be further differentiated by considering Li/Cl ratios; chloride is generally conservative except in the cases of halite precipitation or evaporation, while Li can be added or removed during groundwater flow by mineral interaction and clay formation. A plot of δ^7Li vs. Li/Cl for oil and gas produced waters measured to date (Fig. 9) indicates that shale-hosted formation waters tend to have lower δ^7Li and higher Li/Cl than most sandstone- or carbonate-hosted waters, perhaps reflecting interaction with terrigenous material such as the shale itself (Macpherson et al., 2014). Most produced waters fall within a continuous range that can be explained by evaporated seawater (possibly past halite saturation) mixing with a high Li/Cl, presumably terrigenous, source (Fig. 9). While the Permian Basin produced waters from this study fall well within the range of δ^7Li and Li/Cl for other produced waters, previous work suggests that they represent meteoric waters that inherited the bulk of their dissolved solids from evaporite dissolution (Stueber et al., 1998; Barnaby et al., 2004), which would tend to push Li/Cl ratios toward lower values. This would imply that the San Andres carbonate-hosted formation waters extracted Li from terrestrial sources before, during, and/or after dissolution of marine evaporites, and that they did not have a direct (Permian) seawater source.

In summary, the δ^7Li values in San Andres produced waters are likely not inherited primarily from Permian Type I (marine) evaporites. However, Type II evaporites and associated sediments are plausible sources of Li, especially if hydrothermal processes caused Li enrichment during deposition. The presence of volcanogenic sediments (bentonites) suggest a Li-enriched volcanogenic source is possible. Later interactions with clays and other silicate minerals, either in the present host formation or during migration of the formation waters, could also increase Li concentrations and affect δ^7Li in the produced waters, although host carbonates likely would not have made a significant contribution.

5.3. Lithium sources in shallower groundwaters

The overlap in δ^7Li values between San Andres formation waters and Ogallala aquifer waters provides the possibility that these disparate water systems share a common source of Li. While Permian salts are stratigraphically below the Tertiary Ogallala aquifer, Neogene uplift provided deep groundwater recharge to the west (Bassett and Bentley, 1982; Senger and Fogg, 1987; Senger et al., 1987), and may have allowed eastward erosion of Permian evaporites into the Ogallala recharge area, providing a source for the extensive playa deposits. Percolation of water through playa lake bottoms during wet periods would result in dissolution of soluble salts and transport into the Ogallala aquifer (Nativ, 1992). During this process, Li ultimately derived from Permian evaporites (most likely "Type II" continental evaporites; Lowenstein, 1988) would be delivered to the shallow aquifer system, giving it a signature similar to that of the San Andres produced waters. The Ogallala well water samples show a possible depth stratification of δ^7Li, with the three deepest wells (C1, C3 and C5; Table 3) yielding values of +13.3 to +16.5‰, while the two shallower wells (C2 and

C6) yielded values of +10.6 to +12.5‰. This points to a variable contribution from water-silicate interaction resulting from discontinuities within the aquifer (i.e., isolated lenses) or water chemistry gradients. The trend of heavier δ^7Li with depth is consistent with a greater amount of fluid-silicate interaction (possibly a longer residence time) deeper in the reservoir (Liu et al., 2015). This interpretation is further supported by a positive correlation between δ^7Li and Si concentration in the Ogallala aquifer water (R^2 = 0.77; not shown).

The Santa Rosa Formation lies between the San Andres Formation and the Ogallala aquifer, yet it contains Li with a very different isotopic composition than either (Fig. 4). Because it overlies the main Permian evaporite units, it most likely did not experience the meteoric water invasion that affected the Permian evaporite units during recharge and subsurface flow. Scanlon et al. (2009) suggest exchange of Dockum (Santa Rosa) and Southern High Plains (Ogallala) waters in this region. However, distinctly different δ^7Li values of these groundwaters (Fig. 4) indicate that interaction was minimal at the site of the present study. We note that the chemistry of the two samples from the Santa Rosa well, dominated by Na and SO_4 with TDS values between those of the San Andres Formation and Ogallala aquifer, differs significantly from those two units (Fig. 3), and it also falls well off the halite dissolution/seawater evaporation trend (Fig. 7). Therefore, the δ^7Li of Santa Rosa waters is more likely to reflect interaction of meteoric waters with the clastic component of the unit itself. The relatively high δ^7Li values of waters from this unit could have been imparted by long term fluid-rock interaction, which tends to enrich the fluid in isotopically heavy Li (Chan et al., 1992; Rudnick et al., 2004; Williams and Hervig, 2005; Vigier et al., 2008; Liu et al., 2015).

5.4. Potential contamination of groundwater from brines

The major cation and anion trends from Ogallala groundwater samples in this study are comparable to other data from the southern High Plains aquifer (Mehta et al., 2000; Fryar et al., 2001; Fahlquist, 2003; Scanlon et al., 2009), generally falling on the low-Ca and low-carbonate end of the spectrum. Chaudhuri and Ale (2014) attributed increased salinization and nitrate contamination of Ogallala aquifer groundwater in Texas between 1960 and 2010 to natural processes such as percolation through playas, as well as to agricultural and hydrocarbon exploration activities that can result in mixing with high TDS water from underlying units. For example, the upward migration of these saline waters has been exacerbated in some areas by high-capacity wells used for irrigation (Gurdak et al., 2009). Enhanced oil recovery and CO_2 injection for geologic carbon sequestration both involve increasing the local pressure of the San Andres formation and carry risks of inducing flow of deep brines to shallower levels through faults or existing wellbore penetrations. Thus, it is important to develop geochemical tools that can sensitively detect upward movement of brines in time to prevent significant contamination. The extent to which δ^7Li can serve as a monitor for brine migration or leakage in any given situation depends on regional geologic and hydrologic conditions (cf. Warner et al., 2014), and requires collection and analysis of baseline values for all possible end members.

The overlap in δ^7Li values of Ogallala groundwater within the study area with produced waters from San Andres EOR wells could indicate a contribution from deeper sources. Contamination from drilling activities would have taken place over a relatively short (≤several decades) time scale, during which Li could be expected to behave conservatively. However, the observed linear trends of Ogallala aquifer water δ^7Li values, when plotted against 1/Li in a mixing diagram (Fig. 10), do not point toward either San Andres produced waters or Santa Rosa groundwater as potential high-[Li] end members. These data, combined with significant differences in Li/Cl (Fig. 4) and Cl/Br (Fig. 7) between the San Andres and Ogallala waters, argues against either upward migration of formation waters or downward percolation of released oilfield produced water into the Ogallala aquifer as a significant contributing factor to the higher TDS Ogallala waters at this location.

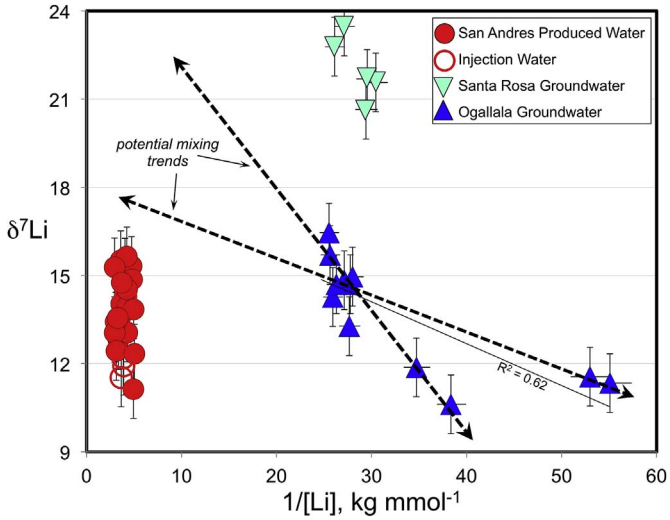

Fig. 10. Mixing diagram depicting two possible trajectories for formation water mixing to explain [Li] vs. δ^7Li trends. In this diagram, a mixing trend would be a straight line from the Ogallala endmember to either a Santa Rosa or a San Andres endmember. One trajectory is anchored by the lowest measured Ogallala δ^7Li water sample, and the other by the lowest [Li] (highest 1/[Li]) Ogallala water sample. In both cases, the trajectory does not point toward either Santa Rosa groundwater or San Andres produced water. The solid line with R^2 = 0.62 is a best-fit line for all of the Ogallala groundwater data.

At the East Seminole site, the intermediate Santa Rosa groundwater provides a monitoring point for possible upward movement of San Andres brines during EOR. While the Ogallala and San Andres waters have essentially identical δ^7Li values, the large difference in δ^7Li between Santa Rosa and San Andres waters makes Li isotopes a sensitive monitor for incursion of the deeper brines. Based on measured δ^7Li and [Li] values, the influx of a relatively small fraction (≤5%) of San Andres water would produce a measurable shift in δ^7Li (≥2‰) in Santa Rosa groundwater (Fig. 5). Thus, monitoring of Santa Rosa groundwater could provide an early warning before brines reach the more sensitive overlying Ogallala aquifer.

6. Conclusions

δ^7Li values (+10.9‰ to +15.6‰) for produced waters from the San Andres Formation carbonate-hosted oil reservoir in the Permian Basin East Seminole field fall within the range of produced waters from other sandstone- and carbonate-hosted oil and gas reservoirs (Chan et al., 2002; Millot et al., 2011; Macpherson et al., 2014; Warner et al., 2014; Phan et al., 2016), but are generally higher than values obtained from hydraulically fractured shale gas wells in the Appalachian Basin, including the Marcellus Shale. While most produced water Li isotope trends can be explained by mixing of deeply evaporated ancient seawater with terrestrially-derived Li, the geologic setting and major element chemistry of San Andres Formation produced waters suggests that their TDS load was derived from dissolution of Permian evaporites by Neogene meteoric water (Stueber et al., 1998; Barnaby et al., 2004). Sources of Li for San Andres produced waters could include (1) interaction of infiltrating meteoric water with Permian continentally-derived evaporite units, (2) interaction of diagenetic fluids with bentonite beds in the stratigraphic section, and/or (3) interaction of fluids with clays and other minerals in the flow path. Neither Permian marine evaporites nor the dolomitic host unit was likely a significant contributor to the total Li load.

Ogallala aquifer groundwater chemistry in the study area is comparable to that of other Southern High Plains aquifer waters. The δ^7Li values of the Ogallala aquifer (+10.6 to +16.5‰) could be inherited from playa lakes in their recharge area. The salts in these lakes are

derived in part from eroded Permian sediments that may impart a Li isotopic signature similar to that of the San Andres produced waters. The intermediate depth Santa Rosa groundwater aquifer lies above Permian evaporites and, considering its significantly different chemistry and isotope composition, likely has not experienced significant infiltration by water from the overlying Ogallala aquifer or underlying San Andres Formation. Therefore, the elevated Santa Rosa groundwater Li isotope composition (+20.6 to +23.5‰) reflects prolonged interaction with clay and other silicate minerals in the aquifer. The hydrology inferred from Li isotope variations is broadly consistent with the geologic and hydrologic history of the area (e.g., Bein and Dutton, 1993; Stueber et al., 1998; Barnaby et al., 2004), and could be further tested by analysis of Permian marine and continental evaporite units and playa salt flats in this region.

A major consideration for the selection of stratigraphic zones for CO_2 injection is the potential migration of CO_2 or displaced saline formation waters into shallow aquifers that could result in the degradation of groundwater quality via salinization and the mobilization of metals and other chemical species. In addition to its use as a natural tracer of groundwater-brine mixing and water-rock interactions, the δ^7Li composition of deep groundwater has potential as a monitoring tool to identify CO_2 injection-induced fluid migration into overlying permeable units prior to its intrusion into sensitive shallow aquifers. Although δ^7Li values of San Andres oilfield waters overlap with those of groundwater from the Ogallala aquifer, δ^7Li of waters from both units are distinct from Santa Rosa groundwater that lies between the two. Thus, a shift in the δ^7Li of groundwater from wells tapping the Santa Rosa aquifer could be used to detect upward fluid migration.

Disclaimer

This project was funded by the Department of Energy, National Energy Technology Laboratory, an agency of the United States Government, through a support contract with URS Energy & Construction, Inc. Neither the United States Government nor any agency thereof, nor any of their employees, nor URS Energy & Construction, Inc., nor any of their employees, makes any warranty, expressed or implied, or assumes any legal liability or responsibility for the accuracy, completeness, or usefulness of any information, apparatus, product, or process disclosed, or represents that its use would not infringe privately owned rights. Reference herein to any specific commercial product, process, or service by trade name, trademark, manufacturer, or otherwise, does not necessarily constitute or imply its endorsement, recommendation, or favoring by the United States Government or any agency thereof. The views and opinions of authors expressed herein do not necessarily state or reflect those of the United States Government or any agency thereof.

Acknowledgements

The authors would like to thank John Saenz and Todd Cox with Tabula Rasa Energy for site access and aid in sample collection at the field site in Texas; Burt Thomas for helpful comments on an earlier draft of the manuscript; and two anonymous reviewers for careful and thorough reviews of the submitted manuscript. Field access and site sampling was conducted under a MOU between NETL and Blue Strategies, LLC. This effort was performed in support of the National Energy Technology Laboratory's ongoing research in Carbon Storage under RES contract DE-FE0004000 (RCC, BWS).

References

Araoka, D., Kawahata, H., Takagi, T., Watanabe, Y., Nishimura, K., Nishio, Y., 2013. Lithium and strontium isotopic systematics in playas in Nevada, USA: constraints on the origin of lithium. Min. Deposita 49, 371–379.

Bachu, S., 2008. CO_2 storage in geological media: role, means, status and barriers to deployment. Prog. Energy Combust. Sci. 34, 254–273.

Bagard, M.-L., West, A.J., Newman, K., Basu, A.R., 2015. Lithium isotope fractionation in the Ganges–Brahmaputra floodplain and implications for groundwater impact on seawater isotopic composition. Earth Planet. Sci. Lett. 432, 404–414.

Banner, J.L., 2004. Radiogenic isotopes: systematics and applications to earth surface processes and chemical stratigraphy. Earth Sci. Rev. 65, 141–194.

Barnaby, R.J., Oetting, G.C., Gao, G., 2004. Strontium isotopic signatures of oil-field waters: applications for reservoir characterization. AAPG Bull. 88, 1677–1704.

Bassett, R.L., Bentley, M.E., 1982. Geochemistry and hydrodynamics of the deep formation brines in the Palo Duro and Dalhart Basins, Texas, USA. J. Hydrol. 59, 331–372.

Bebout, G.E., Carlson, W.D., 1987. Fluid evolution and transport during metamorphism: evidence from the Llano Uplift, Texas. Contrib. Mineral. Pet. 92, 518–529.

Bein, A., Dutton, A.R., 1993. Origin, distribution, and movement of brine in the Permian Basin (U.S.A.): a model for displacement of connate brine. Geol. Soc. Am. Bull. 105, 695–707.

California Department of Public Health, 2010. Drinking Water Notification Levels and Response Levels, an Overview. California Department of Public Health Drinking Water Program. http://www.cdph.ca.gov/certlic/drinkingwater/Documents/Notificationlevels/notificationlevels.pdf (accessed February 2017).

Carroll, S., Hao, Y., Aines, R., 2010. Geochemical detection of carbon dioxide in dilute aquifers. Geochem. Trans. 10. http://dx.doi.org/10.1186/1467-4866-10-4.

Chan, L.-H., Starinsky, A., Katz, A., 2002. The behavior of lithium and its isotopes in oilfield brines: evidence from the Heletz–Kokhav field, Israel. Geochim. Cosmochim. Acta 66, 615–623.

Chan, L.H., Edmond, J.M., Thompson, G., Gillis, K., 1992. Lithium isotopic composition of submarine basalts: implications for the lithium cycle in the oceans. Earth Planet. Sci. Lett. 108, 151–160.

Chapman, E.C., Capo, R.C., Stewart, B.W., Kirby, C.S., Hammack, R.W., Schroeder, K.T., Edenborn, H.M., 2012. Geochemical and strontium isotope characterization of produced waters from Marcellus Shale natural gas extraction. Environ. Sci. Technol. 46, 3545–3553.

Chaudhuri, S., Ale, S., 2014. Long term (1960–2010) trends in groundwater contamination and salinization in the Ogallala aquifer in Texas. J. Hydrol. 513, 376–390.

Chaudhuri, S., Furlan, S., Clauer, N., 1992. The signature of water-rock interactions in the formation waters of sedimentary basins: some new evidence. In: Kharaka, Y.K., Maest, A.S. (Eds.), Water-Rock Interaction 2. A. A. Balkema, Rotterdam, pp. 907–910.

Choi, M.S., Ryu, J.-S., Park, H.Y., Lee, K.-S., Kil, Y., Shin, H.S., 2013. Precise determination of the lithium isotope ratio in geological samples using MC-ICP-MS with cool plasma. J. Anal. At. Spectrom. 28, 505–509.

Collins, A.G., 1975. Geochemistry of Oilfield Waters. Elsevier, New York, pp. 496.

Dellinger, M., Gaillardet, J., Bouchez, J., Calmels, D., Galy, V., Hilton, R.G., Louvat, P., France-Lanord, C., 2014. Lithium isotopes in large rivers reveal the cannibalistic nature of modern continental weathering and erosion. Earth Planet. Sci. Lett. 401, 359–372.

DOE-NETL, 2010. Carbon dioxide Enhance Oil Recovery: Untapped Domestic Energy Supply and Long Term Carbon Storage Solution. Department of Energy - National Energy Technology Laboratory. https://www.netl.doe.gov/file%20library/research/oil-gas/small_CO2_EOR_Primer.pdf.

Dutton, A.R., 1987. Origin of brine in the San Andres Formation, evaporite confining system, Texas Panhandle and eastern New Mexico. Geol. Soc. Am. Bull. 99, 103–112.

Dutton, S.P., Kim, E.M., Broadhead, R.F., Raatz, W.D., Breton, C.L., Ruppel, S.C., Kerans, C., 2005. Play analysis and leading-edge oil-reservoir development methods in the Permian basin: increased recovery through advanced technologies. AAPG Bull. 89, 553–576.

Engle, M.A., Blondes, M.S., 2014. Linking compositional data analysis with thermodynamic geochemical modeling: oilfield brines from the Permian Basin, USA. J. Geochem. Explor. 141, 61–70.

Engle, M.A., Reyes, F.R., Varonka, M.S., Orem, W.H., Ma, L., Ianno, A.J., Schell, T.M., Xu, P., Carroll, K.C., 2016. Geochemistry of formation waters from the Wolfcamp and "Cline" shales: insights into brine origin, reservoir connectivity, and fluid flow in the Permian Basin, USA. Chem. Geol. 425, 76–92.

Fahlquist, L., 2003. Ground-water Quality of the Southern High Plains Aquifer, Texas and New Mexico, 2001. pp. 1–69 U.S. Geol. Surv. Open-File Report 03-345.

Fryar, A.E., Mullican, W.F., Macko, S.A., 2001. Groundwater recharge and chemical evolution in the southern High Plains of Texas, USA. Hydrogeol. J. 9, 522–542.

Godec, M.L., Kuuskraa, V.A., Dipietro, P., 2013. Opportunities for using anthropogenic CO_2 for enhanced oil recovery and CO_2 storage. Energy Fuels 27, 4183–4189.

Godfrey, L.V., Chan, L.-H., Alonso, R.N., Lowenstein, T.K., McDonough, W.F., Houston, J., Li, J., Bobst, A., Jordon, T.E., 2013. The role of climate in the accumulation of lithium-rich brine in the Central Andes. Appl. Geochem. 38, 92–102.

Gray, T.J., 1989. East Seminole San Andres Field, Gaines County, Texas. Development Study for Mobil Exploration & Producing U.S. Inc., Midland Division, pp. 46.

Gurdak, J.J., McMahon, P.B., Dennehy, K.F., Qi, S.L., 2009. Water quality in the high Plains aquifer, Colorado, Kansas, Nebraska, New Mexico, Oklahoma, South Dakota, Texas, and Wyoming, 1999-2004. U.S. Geol. Surv. Circ. 1337, 46.

Haluszczak, L.O., Rose, A.W., Kump, L.R., 2013. Geochemical evaluation of flowback brine from Marcellus gas wells in Pennsylvania, USA. Appl. Geochem 28, 55–61.

Hanor, J.S., 1994. Origin of saline fluids in sedimentary basins. In: Parnell, J. (Ed.), Origin and Migration of Fluids in Sedimentary Basins, Special Publication 78. Geological Society, London, pp. 151–174.

Hermann, A.G., 1980. Bromide distribution between halite and NaCl-saturated seawater. Chem. Geol. 28, 171–177.

Hopkins, J., 1993. Water-quality Evaluation of the Ogallala Aquifer, Texas. Texas Water Development Board Report, pp. 40.

Hornbeck, R., Keskin, P., 2014. The historically evolving impact of the Ogallala aquifer: agricultural adaptation to groundwater and drought. Am. Econ. J. Appl. Econ. 6,

190–219.
Kharaka, Y.K., Hanor, J.S., 2004. Deep fluids in the continents: I. Sedimentary basins. In: Drever, J.I. (Ed.), Treatis on Geochemistry. Surface and Ground Water, Weathering and Soils, vol. 5. Elsevier Pergamon, pp. 499–540.
Kloppmann, W., Chikurel, H., Picot, G., Guttman, J., Pettenati, M., Aharoni, A., Guerrot, C., Millot, R., Gaus, I., Wintgens, T., 2009. B and Li isotopes as intrinsic tracers for injection tests in aquifer storage and recovery systems. Appl. Geochem. 24, 1214–1223.
Kolesar Kohl, C.A., Capo, R.C., Stewart, B.W., Wall, A.J., Schroeder, K.T., Hammack, R.W., Guthrie, G.D., 2014. Strontium isotopes test long-term zonal isolation of injected and Marcellus Formation water after hydraulic fracturing. Environ. Sci. Technol. 48, 9867–9873.
Land, L.S., Macpherson, G.L., 1992. Origin of saline formation waters, Cenozoic section, Gulf of Mexico sedimentary basin. AAPG Bull. 76, 1344–1362.
Land, L.S., Prezbindowski, D.R., 1981. The origin and evolution of saline formation water, Lower Cretaceous carbonates, south-central Texas, USA. J. Hydrol. 54, 51–74.
Li, Y.-H., 1991. Distribution patterns of the elements in the ocean: a synthesis. Geochim. Cosmochim. Acta 55, 3223–3240.
Lin, J., Liu, Y., Hu, Z., Yang, L., Chen, K., Chen, H., Zong, K., Gao, S., 2016. Accurate determination of lithium isotope ratios by MC-ICP-MS without strict matrix-matching by using a novel washing method. J. Anal. At. Spectrom. 31, 390–397.
Liu, X.-M., Wanner, C., Rudnick, R.L., McDonough, W.F., 2015. Processes controlling δ^7Li in rivers illuminated by study of streams and groundwaters draining basalts. Earth Planet. Sci. Lett. 409, 212–224.
Lowenstein, T.K., 1988. Origin of depositional cycles in a Permian "saline giant": the Salado (McNutt zone) evaporites of New Mexico and Texas. Geol. Soc. Am. Bull. 100, 592–608.
Macpherson, G.L., Capo, R.C., Stewart, B.W., Phan, T.T., Schroeder, K.T., Hammack, R.W., 2014. Temperature-dependent Li isotope ratios in Appalachian Plateau and Gulf Coast Sedimentary Basin saline water. Geofluids 14, 419–429.
Magruder, J.B., Stiles, L.H., Yelverton, T.D., 1990. Review of the means San Andes unit CO_2 tertiary project. J. Pet. Technol. 42, 638–644.
Manrique, E., Gurfinkel, M., Muci, V., 2004. Enhanced oil recovery field experiences in carbonate reservoirs in the United States. In: 25th Annual Workshop & Symposium Collaborative Project on Enhanced Oil Recovery. International Energy Agency, Stavanger, Norway, pp. 1–32.
Marriott, C.S., Henderson, G.M., Crompton, R., Staubwasser, M., Shaw, S., 2004. Effect of mineralogy, salinity, and temperature on Li/Ca and Li isotope composition of calcium carbonate. Chem. Geol. 212, 5–15.
McCaffrey, M.A., Lazar, B., Holland, H.D., 1987. The evaporation path of seawater and the coprecipitation of Br^- and K^+ with halite. J. Sed. Res. 57, 928–937.
Mehta, S., Fryar, A.E., Banner, J.L., 2000. Controls on the regional-scale salinization of the Ogallala aquifer, southern high Plains, Texas, USA. Appl. Geochem. 15, 849–864.
Meredith, K., Moriguti, T., Tomascak, P.B., Hollins, S., Nakamura, E., 2013. The lithium, boron and strontium isotopic systematics of groundwaters from an arid aquifer system: implications for recharge and weathering processes. Geochim. Cosmochim. Acta 112, 20–31.
Merrill, M.D., Slucher, E.R., Roberts-Ashby, T.L., Warwick, P.D., Blondes, M.S., Freeman, P.A., Cahan, S.M., DeVera, C.A., Lohr, C.D., 2015. Geologic framework for the national assessment of carbon dioxide storage resources - Permian and Palo Duro Basins and Bend Arch-Fort Worth Basin (chapter K). In: Warwick, P.D., Corum, M.D. (Eds.), Geologic Framework for the National Assessment of Carbon Dioxide Storage Resources, pp. 1–42 U.S. Geological Survey Open-File Report 2012-1024-K.
Millero, F.J., Sohn, M.L., 1992. Chemical Oceanography. CRC Press, Boca Raton FL, pp. 531.
Millot, R., Guerrot, C., Innocent, C., Négrel, P., Sanjuan, B., 2011. Chemical, multi-isotopic (Li–B–Sr–U–H–O) and thermal characterization of Triassic formation waters from the Paris Basin. Chem. Geol. 283, 226–241.
Millot, R., Hegan, A., Négrel, P., 2012. Geothermal waters from the Taupo volcanic zone, New Zealand: Li, B and Sr isotopes characterization. Appl. Geochem. 27, 677–688.
Millot, R., Vigier, N., Gaillardet, J., 2010. Behaviour of lithium and its isotopes during weathering in the Mackenzie Basin, Canada. Geochim. Cosmochim. Acta 74, 3897–3912.
Minnesota Department of Health, 2013. Human Health-based Water Guidance Table. http://www.health.state.mn.us/divs/eh/risk/guidance/gw/table.html (accessed February 2017).
Misra, S., Froelich, P.N., 2012. Lithium isotope history of Cenozoic seawater: changes in silicate weathering and reverse weathering. Science 335, 818–823.
Nativ, R., 1992. Recharge into southern high Plains aquifer - possible mechanisms, unresolved questions. Environ. Geol. Water Sci. 19, 21–32.
Nishio, Y., Nakai, S., 2002. Accurate and precise lithium isotopic determinations of igneous rock samples using multi-collector inductively coupled plasma mass spectrometry. Anal. Chim. Acta 456, 271–281.
Phan, T.T., Capo, R.C., Stewart, B.W., Macpherson, G.L., Rowan, E.L., Hammack, R.W., 2016. Factors controlling Li concentration and isotopic composition in formation waters and host rocks of Marcellus Shale. Appalach. Basin. Chem. Geol. 420, 162–179.
Pogge von Strandmann, P.A.E., Burton, K.W., James, R.H., van Calsteren, P., Gislason, S.R., 2010. Assessing the role of climate on uranium and lithium isotope behaviour in rivers draining a basaltic terrain. Chem. Geol. 270, 227–239.
Pogge von Strandmann, P.A.E., Frings, P.J., Murphy, M.J., 2017. Lithium isotope behaviour during weathering in the Ganges Alluvial Plain. Geochim. Cosmochim. Acta 198, 17–31.
Pogge von Strandmann, P.A.E., Jenkyns, H.C., Woodfine, R.G., 2013. Lithium isotope evidence for enhanced weathering during Oceanic Anoxic Event 2. Nat. Geosci. 6, 668–672.
Potratz, V.Y., 1980. Ground-water Geochemistry of the Ogallala Aquifer in the Southern High Plains of Texas and New Mexico. M.S. Thesis. Texas Tech University, pp. 119.
Ramondetta, P.J., 1982. Facies and Stratigraphy of the San Andres Formation, Northern and Northwestern Shelves of the Midland Basin, Texas and New Mexico. Bureau of Economic Geology Report of Investigations no. 128. The University of Texas at Austin, pp. 56.
Rettman, P.L., Leggat, E.R., 1966. Ground-water resources of Gaines County, Texas: Texas Water Development Board & U.S. Geol. Survey Report 15pp. 176.
Romanak, K.D., Smyth, R.C., Yang, C., Hovorka, S.D., Rearick, M., Lu, J., 2012. Sensitivity of groundwater systems to CO_2: application of a site-specific analysis of carbonate monitoring parameters at the SACROC CO_2-enhanced oil field. Int. J. Greenh. Gas. Contr. 6, 142–152.
Rudnick, R.L., Tomascak, P.B., Njo, H.B., Gardner, L.R., 2004. Extreme lithium isotopic fractionation during continental weathering revealed in saprolites from South Carolina. Chem. Geol. 212, 45–57.
Ruppel, S.C., Cander, H.S., 1988. Dolomitization of shallow-water platform carbonates by sea water and seawater-derived brines: San Andres Formation (Guadalupian), west Texas. In: Shukla, V., Baker, P.A. (Eds.), Sedimentology and Geochemistry of Dolostones. SEPM Special Publication 43, Society of Economic Paleontologists and Mineralogists, pp. 245–262.
Scanlon, B.R., Nicot, J.P., Reedy, R.C., Kurtzman, D., Mukherjee, A., Nordstrom, D.K., 2009. Elevated naturally occurring arsenic in a semiarid oxidizing system, Southern High Plains aquifer, Texas, USA. Appl. Geochem. 24, 2061–2071.
Senger, R.K., Fogg, G.E., 1987. Regional underpressuring in deep brine aquifers, Palo Duro Basin, Texas 1. Effects of hydrostratigraphy and topography. Water Resour. Res. 23, 1481–1493.
Senger, R.K., Kreitler, C.W., Fogg, G.E., 1987. Regional underpressuring in deep brine aquifers, Palo Duro Basin, Texas: 2. The effect of Cenozoic basin development. Water Resour. Res. 23, 1494–1504.
Smith, G.I., Barczak, V.J., Moulton, G.F., Liddicoat, J.C., 1983. Core KM-3, a Surface-to Bedrock Record of Late Cenozoic Sedimentation in Searles Valley, California. pp. 1–73 U.S. Geol. Surv. Prof. Paper 1256.
Smyth, R.C., Hovorka, S.D., Lu, J., Romanak, K.D., Partin, J.W., Wong, C., Yang, C., 2009. Assessing risk to fresh water resources from long term CO_2 injection – laboratory and field studies. Energy Procedia 1, 1957–1964.
Stanton, J.S., Fahlquist, L., 2006. Ground-water quality beneath irrigated cropland of the northern and southern High Plains Aquifer, Nebraska and Texas, 2003–04. U.S. Geol. Surv. Sci. Invest. Rep. 2006–5196, 1–94.
Stevens, S.H., Kuuskraa, V.A., Gale, J., Beecy, D., 2001. CO_2 injection and sequestration in depleted oil and gas fields and deep coal seams: worldwide potential and costs. Environ. Geosci. 8, 200–209.
Stewart, B.W., Capo, R.C., Chadwick, O.A., 1998. Quantitative strontium isotope models for weathering, pedogenesis and biogeochemical cycling. Geoderma 82, 173–195.
Stoessell, R.K., Carpenter, A.B., 1986. Stoichiometric saturation tests of $NaCl_{1-x}Br_x$ and $KCl_{1-x}Br_x$. Geochim. Cosmochim. Acta 50, 1465–1474.
Stueber, A.M., Saller, A.H., Ishida, H., 1998. Origin, migration, and mixing of brines in the Permian basin: geochemical evidence from the eastern Central Basin platform, Texas. AAPG Bull. 82, 1652–1672.
Tennyson, M.E., Cook, T.A., Charpentier, R.R., Gautier, D.L., Klett, T.R., Verma, M.K., Ryder, R.T., Attanasi, E.D., Freeman, P.A., Le, P.A., 2012. Assessment of Remaining Recoverable Oil in Selected Major Oil Fields of the Permian Basin, Texas and New Mexico. pp. 4 U.S. Geol. Surv. Fact Sheet 2012-3051.
Tipper, E.T., Calmels, D., Gaillardet, J., Louvat, P., Capmas, F., Dubacq, B., 2012. Positive correlation between Li and Mg isotope ratios in the river waters of the Mackenzie Basin challenges the interpretation of apparent isotopic fractionation during weathering. Earth Planet. Sci. Lett. 333–334, 35–45.
Todd, R.G., 1976. Oolite-bar progradation, San Andres Formation, Midiand basin, Texas. AAPG Bull. 60, 907–925.
Tomascak, P.B., Hemming, N.G., Hemming, S.R., 2003. The lithium isotopic composition of waters of the Mono Basin, California. Geochim. Cosmochim. Acta 67, 601–611.
Tomascak, P.B., Magna, T., Dohmen, R., 2016. Advances in Lithium Isotope Geochemistry. Springer International Publishing, Cham, Switzerland, pp. 195.
Venkataraman, K., Uddameri, V., 2012. Modeling simultaneous exceedance of drinking-water standards of arsenic and nitrate in the Southern Ogallala aquifer using multinomial logistic regression. J. Hydrol. 458–459, 16–27.
Vigier, N., Decarreau, A., Millot, R., Carignan, J., Petit, S., France-Lanord, C., 2008. Quantifying Li isotope fractionation during smectite formation and implications for the Li cycle. Geochim. Cosmochim. Acta 72, 780–792.
Walter, L.M., Steuber, A.M., Huston, T.J., 1990. Br-Cl-Na systematics in Illinois basin fluids constraints on fluid origin and evolution. Geology 18, 315–318.
Wang, F.P., Lucia, F.J., Kerans, C., 1998. Integrated reservoir characterization study of a carbonate ramp reservoir: Seminole San Andres unit, Gaines County, Texas. SPE Reserv. Eval. Eng. 105–113.
Ward, R.F., Kendall, C.G.S.C., Harris, P.M., 1986. Upper Permian (Guadalupian) facies and their association with hydrocarbons - Permian basin, west Texas and New Mexico. AAPG Bull. 70, 239–262.
Warner, N.R., Darrah, T.H., Jackson, R.B., Millot, R., Kloppmann, W., Vengosh, A., 2014. New tracers identify hydraulic fracturing fluids and accidental releases from oil and

gas operations. Environ. Sci. Technol. 48, 12552–12560.
Williams, L.B., Clauer, N., Hervig, R.L., 2012. Light stable isotope microanalysis of clays in sedimentary rocks. In: Sylvester, P.J. (Ed.), Quantitative Mineralogy and Microanalysis of Sediments and Sedimentary Rocks. Mineralogical Association of Canada Short Course 42, pp. 55–73.
Williams, L.B., Elliott, W.C., Hervig, R.L., 2015. Tracing hydrocarbons in gas shale using lithium and boron isotopes: Denver Basin USA, Wattenberg gas field. Chem. Geol. 417, 404–413.
Williams, L.B., Hervig, R.L., 2005. Lithium and boron isotopes in illite-smectite: the importance of crystal size. Geochim. Cosmochim. Acta 69, 5705–5716.
Williams, L.B., Środoń, J., Huff, W.D., Clauer, N., Hervig, R.L., 2013. Light element distributions (N, B, Li) in Baltic Basin bentonites record organic sources. Geochim. Cosmochim. Acta 120, 582–599.
Wilson, T.P., Long, D.T., 1993. Geochemistry and isotope chemistry of Michigan Basin brines: Devonian formations. Appl. Geochem. 8, 81–100.